Journal of the Korean Nuclear Society
Volume 25, Number 1, March 1993

Measurements of Void Concentration Parameters in the Drift-Flux Model

B.J. Yun, G.C. Park and C.H. Chung
Seoul National University
(Received August 6, 1992)

상대유량 모델내의 기포분포계수 측정에 관한 연구

윤병조 · 박군철 · 정창현
서울대학교
(1992. 8. 6 접수)

Abstract

To predict accurately the thermal hydraulic behavior of light water reactors during normal or abnormal operation, the accurate estimation of the void distribution is required. Up to date, many techniques for predicting void fraction of two-phase flow systems have been suggested. Among these techniques, the drift-flux model is widely used because of its exact calculation ability and simplicity. However, to get more accurate prediction of void fraction using drift-flux model, slip and flow regime effects must be considered more properly. In the drift-flux method, these two effects are accounted for by two drift-flux parameters ; C_o and $\bar{V}_{gj}$. At earlier stage, C_o is measured in a circular tube. In this study, C_o is experimentally determined by measuring local void fraction and vapor velocity distribution in a rectangular subchannel having 4 heating rods which simulates nuclear subchannels. The measurements are performed with two-electrical conductivity probes which are known to be adequate for measuring local parameters. The experiments are performed at low flow rate and the system pressure less than 3 atmo spheric pressure. In this experiment, $\bar{V}_{gj}$ is not measured, but quoted from well-known empirical correlation to formulate C_o. Finally, C_o is expressed as a function of channel averaged void fraction.

요 약

가압경수로형 원자로의 정상 비정상 운전시의 열수력학적 거동을 예측하기 위해서는 원자로내 기포계수의 분포를 정확히 계산하는 것이 필수적이다.이러한 기포계수의 정확한 예측을 위하여 많은 모델들이 제시되었다. 이중 drift-flux 모델은 그 계산의 정확성과 간결성에 의하여널리 사용되고 있다. 이러한 drift-flux 모델을 사용하여 보다 더 정확한 기포계수를 예측하기 위해서는 각 상간의 슬립률과 flow regime 에 따른 기포의 운동의 변화가 정확히 고려되어야 한다. Drift-flux 모델에서는 이러한 두가지 요소가 drift-flux parameter인 C_o와 $\bar{V}_{gj}$에서 고려된다. 본 연구에서는 이러한 C_o의 실험적 결정을 위하여 원자로 노심을 모사한 4개의 전열봉이 있는 비등이 발생하는 수직사각

유로를 구성하였으며, 완성된 유로내에서 기포계수의 분포 및 기포속도의 분포를 측정하였다. 국부적 기포계수 및 기포속도 분포의 측정에 사용된 방법은 이중탐침법이며 측정이 이루어진 유로내의 유동 상태는 유속이 비교적 느린 low flow rate condition이며 유로내 압력은 3기압 이하이다. 본 실험에서는 액상의 속도는 측정되지 않았으며, 따라서 C_o의 계산을 위하여 $\bar{V}_{gj}$의 실험 상관관계식을 사용하여 유로내 평균 기포계수의 함수로 나타내었다.

1. Introduction

Two phase flow phenomena have been studied with many theoretical and experimental methods for various systems in nuclear power plant and related industries. In particular, the exact prediction of void fraction in the subchannel under two phase flow is of great importance to safety analysis of nuclear power plants and verification of thermal-hydraulic design code. Such studies for two phase flow are very difficult to formulate quantitatively due to its complex phenomena. Up to date, many theoretical models for analysis of two phase flow have been developed. Among these models, drift-flux model is widely used because of its simplicity and accuracy. In modeling of a two phase system using the drift-flux model, it is necessary to represent both the relative motion between the phases and the void distribution. These are expressed by averaged and weighted values of the system parameters. But in these treatments, the information on changes of variables in the direction normal to the main flow within channel is lost, therefore the transfer of momentum and energy between phases should be expressed by empirical correlations. Among these correlations, the drift velocity, $\bar{V}_{gj}$, represents the relative velocity of the vapor with respect to hypothetical mixture velocity and the concentration parameter, C_o, is the parameter considering the void distribution. An earlier research shows that C_o is only a function of flow pattern, so in this research C_o is formulated as a function of channel averaged void fraction in the subcooled boiling by measuring local void fractions and vapor velocities. The measurements of local void fractions and vapor velocities are performed with two-electrical conductivity probes. But in this research, liquid velocity is not directly measured so that empirical correlation $\bar{V}_{gj}$ is used to formulate C_o.

2. Theory

The drift-flux model introduced by Zuber & Findley, is to describe the mixture motion instead of individual phasic motion in the two-fluid model. The basic drift parameters are defined as following which describe the relative motion between two phases.[1,2,3,4,5]

$$j_g = \alpha V_g \tag{1}$$

$$j_f = (1-\alpha)V_f \tag{2}$$

$$j = j_f + j_g = (1-\alpha)V_f + \alpha V_g \tag{3}$$

$$V_{gj} = V_g - j \tag{4}$$

where

j_f : superficial liquid velocity

j_g : superficial vapor velocity

j : superficial velocity

V_{gj} : local drift velocity

And the average value of local parameter, F, defined the average on the cross-section area,

$$\langle F\rangle = \frac{1}{A}\int_A F\, dA \tag{5}$$

then mass conservation equation using above average notation, $\langle\ \rangle$, is

$$G_o A = \rho_f \langle j_f\rangle A + \rho_g \langle j_g\rangle A \tag{6}$$

where the notations are conventional, From Equations (5) and (6) superficial liquid velocity is

$$\langle j_f\rangle = \frac{G_o - \rho_g\langle j_g\rangle}{\rho_f} \tag{7}$$

Finally, expression for C_o is obtained from equations (3) and (5) as

$$C_o \equiv \frac{\langle \alpha j \rangle}{\langle \alpha \rangle \langle j \rangle} = \frac{\langle j_g \rangle}{\langle \alpha \rangle \langle j \rangle} - \frac{\bar{V}_{gj}}{\langle j \rangle} \tag{8}$$

where $\bar{V}_{gj}$ is defined as follows

$$\bar{V}_{gj} \equiv \frac{\langle \alpha (V_g - j) \rangle}{\langle \alpha \rangle} \tag{9}$$

and slip ratio, S, and flow qulity, $\langle x \rangle$, are expressed as

$$\langle x \rangle = \frac{\rho_g \langle j_g \rangle}{G} \tag{10}$$

$$S = \frac{\langle u_g \rangle}{\langle u_f \rangle} = \frac{\rho_f \langle x \rangle \langle 1-\alpha \rangle}{\rho_g \langle \alpha \rangle - \rho_g \langle x \rangle \langle \alpha \rangle} \tag{11}$$

In this paper, the following dirft velocity correlation for $\bar{V}_{gj}$ is used to calculate the concentration parameter C_o[4].

$$\bar{V}_{gj} = \frac{2.9 (g g_c \sigma (\rho_f - \rho_g))^{1/4}}{\rho_f^{1/2}} \tag{12}$$

where

g_c : conversion factor

g : gravitational acceleration constant

σ : surface tension

3. Test device

Figure 1 shows a schematic diagram of the test loop. Experimental apparatus consists of a subchannel test section having 4 heating rods, preheater, flow meter, by-pass line, pump, storage tank, and secondary loop. The test channel is designed to be vertical rectangular geometry to simulate the nuclear reactor system. The overall length of test channel is 202.8 cm and the channel cross section having four heating rods is 5 cm $\times$5 cm. The hydraulic diameter is 1.847 cm. The outer diameter of a rod is 15mm and heat output from 4 rods is 40 kw. The preheater consists of five U-shaped electrical heaters and is located at the subchannel entrance. Its total heat output is 50 kw and the inlet temperature is controlled by a digital temperature controller. In this experiment, the liquid volumetric flow rate is measured by two orifice type flowmeters with wide and narrow range, which are installed between preheater and storage tank. Flow rate is controlled by ball valve and by-pass line connected to the storage tank. Storage tank is composed of water reservoir tank and secondary loop for cooling down of the tank water before flowing into pump. The volume of storage tank is about 300 liters and secondary loop is made of wrinkled stainless steel tube.

4. Double conductivity probe

4.1. Principle of measurements

The principle of two phase flow measurement by the conductivity probe is based upon the electrical resistance difference between the vapor phase and the liquid phase. In a vapor-water flow, the vapor phase can be considered as electrically insulated, whereas the liquid phase as electrically conducting. When the conductivity probe contacts with the continuous liquid, the circuit is closed. But a vapor will break the circuit. Thus the probe works like a switch yielding a two-state signal. In this study, a double conductivity probe is used to measure both the void fraction and the vapor velocity. Figure 2 shows the schematic diagram of double conductivity probe. If the distance between the start probe and the stop probe is too long, probability that a vapor which contacts the start probe can also contact the stop probe will decrease. Thus the distance must be adjusted properly. Serizawa has designed the probe distance to be 5 mm, but the distance between start and stop probes in these experiments is about 1 mm in consideration of the characteristic of the test loop and the flow condition. From the analy-

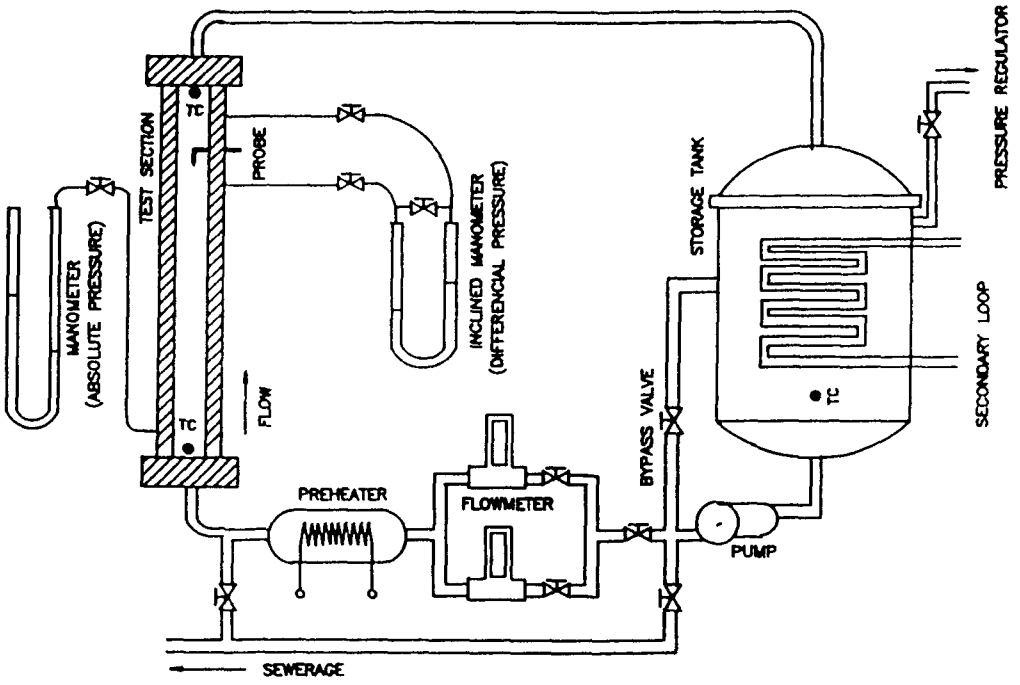

Fig. 1. Schematic Diagram of Test Loop

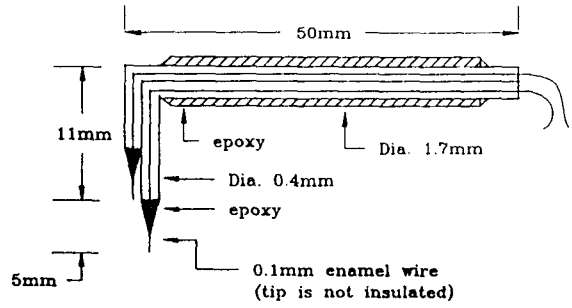

Fig. 2. Schematic Diagram of Double Conductivity Probe

sis of photograph of high speed camera, the probe distance determined in this research is confirmed to be proper. Measurements of probe distance are performed with an electron microscope of the resolution of 1/1000 mm.

4.2. Circuit and data acquisition system

Bridge amplifier circuit is used to convert the resistance difference between two phases into voltage difference. In the experiment, electrical noise is very low and signal to noise ratio is good. But the circuit of low pass filter whose cutoff frequency is 1 Mhz is attached to the bridge amplifier circuit in order to reduce high frequency noise. The double probe and electrical circuits are used in the experiments after calibrated in the air–water pyrex loop. Used A/D converter has 12 bit resolution and its maximum conversion rate is 100 Khz.

5. Calculation of local void fraction and vapor velocity

5.1. Formation of signal

Figure 3 shows hypothetical signal output from double conductivity probe. The formation of signal is affected by surface tension of fluid. If the surface tension of fluid is high then the probe

wetting is minimized so that the generated signal will be rectangular, and if surface tension is low then signal will be formed as in Figure 3 due to probe wetting. In the experiments, distilled water is used so that signal formation is similar to that of Figure 3. Thus the determination of cutoff level which is the boundary between two phases greatly affects calculations of void fraction and vapor velocity.

5.2. Determination of cutoff level

The signal output could not be the form of rectangular sharply as mentioned above due to probe wetting when the probe tip pierces a vapor as shown in Figure 4. Thus the probe tip should be designed to be sharp so that this effect can be minimized. However the determination of cutoff level is very difficult because the interfacial boundary between two phases is not clear even with the sharp tip. In experiments the pacer trigger rate of A/D converter is 5000 hz and data is sampled for 4 secs at each measuring point, that is, the number of the total data is 20000 at each measuring point. In this study,the cutoff level has been determined statistically by VAC (Vapor Analysis Code) with following procedures.

1) Calculate CUT(n) which is average value of every 500 data and repeat this procedure until CUT(n) is converged to just above the level of liquid.
2) Sampling 20 data, 10 data at front and 10 data at rear of the target data point, which are sampled when the data are lower than CUT(n) and the slope of two adjacent data points is lower than optimized value 7.
3) 95 % single ended confidence limit is calculated using above sampled 20 data as follows (it is the cutoff level at each target data point)

$$\text{Cutoff level} = \bar{m} + 2.33\frac{\sigma}{\sqrt{n}} \qquad (13)$$

4) Repeat above step 2 and step 3 for each 20000 data points.
5) Convert raw data into rectangular form by comparision of raw data with cutoff level calculated step 3
6) If converted data at step 5 are higher than CUT(n) then it is considered as vapor and if lower than that then it is considered as liquid (filtering procedure)

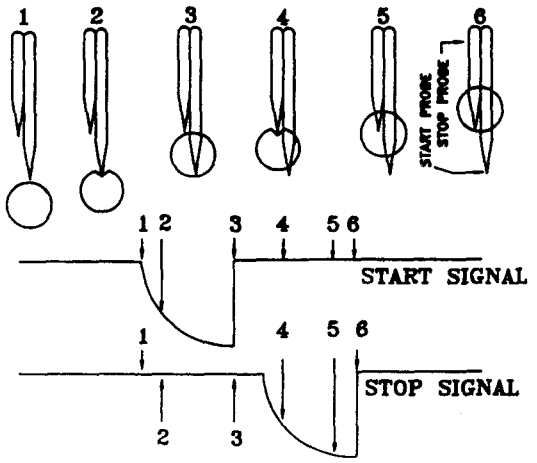

Fig. 3. Hypothetical Signal Output of Double Conductivity Probe

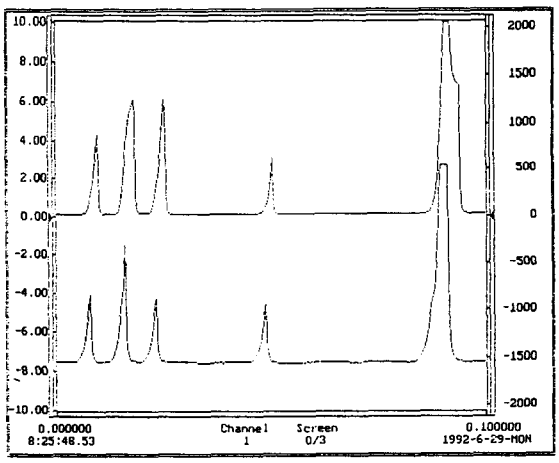

Fig. 4. Signal Output of Double Conductivity Probe at Subchannel

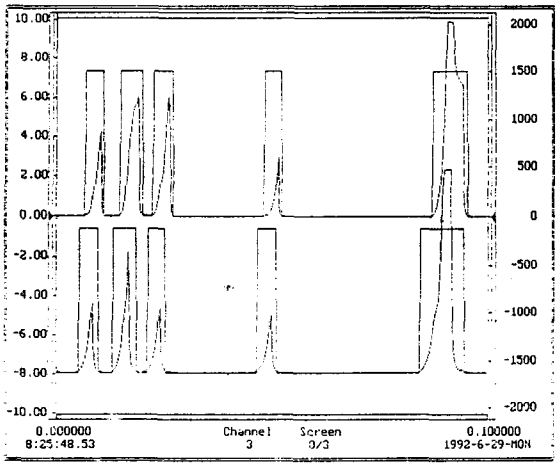

Fig. 5. Converted Signal of Rectangular Form by VAC

Figure 5 shows the converted signal of rectangular form and the signal of the raw data at the same time.

5.3. Calculation of local void fraction

The local void fraction is defined as a time average of the void concentration, f(x,y,t),by

$$\alpha(x,y) = \frac{1}{T}\int_0^T [\,1 - f(x,y,t)\,]\,dt \qquad (14)$$

in which f(x,y,t) equals zero if the phase at the probe tip is vapor and one if liquid. In this study f(x,y,t) is converted signal of start probe by VAC.

5.4. Calculation of vapor velocity

Vapor velocity is calculated by probe distance and time difference between two converted start and stop signals. If ΔZ is probe distance and τ is time difference between two signals, the vapor velocity, V_b, is calculated as follows.

$$V_b = \Delta Z/\tau \qquad (15)$$

Vapor velocity calculated from above equation contains three cases of vapor motions as shown in

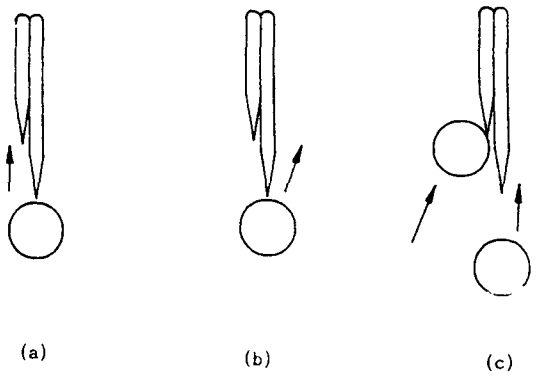

Fig. 6. Three Cases of Vapor Motion at Double Probe

Figure 6. Cases (b),(c) of Figure 6 exist at both ends of velocity distribution function. In this study these two cases are rejected by statistical treatment and the new velocity distribution function is acquired. The following procedures are followed to calculate time averaged velocity by VAC.

1) Calculation of maximum time difference, τ_{max}, by assuming the lowest vapor velocity
2) Calculation of time difference τ between start and stop probes and bubble elapsed time at each probe
3) Time difference is determined by comparision of bubble sizes among them obtained above step 2
4) 99 % double ended confidence limit of time difference is calculated as follows using results of step 3

$$\tau avg - 2.58\frac{\sigma}{\sqrt{n}} \le \tau \le \tau avg + 2.58\frac{\sigma}{\sqrt{n}} \qquad (16)$$

5) New time difference distribution function is obtained by rejection technique using above confidence limit
6) Calculation of average time difference, average vapor velocity and vapor size using new

distribution function

Figure 7 shows the flowchart of VAC.

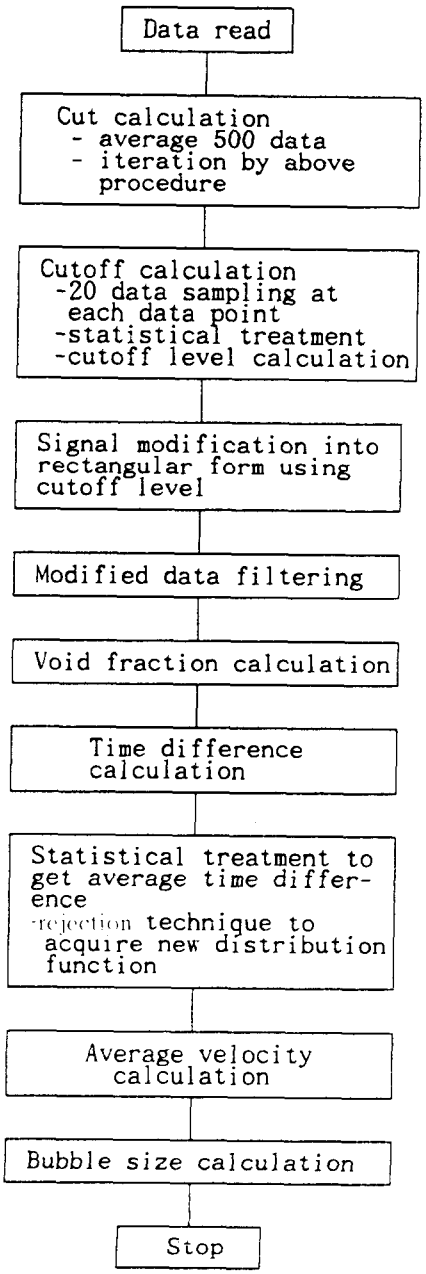

Fig. 7. Flowchart of VAC

6. Measurements and experimental procedure

6.1. Measurements

Measured parameters are system pressure, temperature, mass flow rate, local void fraction and vapor velocity. System pressure is measured with manometer and its measuring point is at the elevation of 131 cm from the bottom of the test channel. Temperatures are measured with k-type thermocouples and their measuring positions are the entrance and the exit of the test channel, and the entrance temperature is maintained constantly by preheater during measurements. Measurements of vapor velocity and void fraction are performed by traversing 4 double conductivity probes mounted on subchannel wall and their axial position is at 164.5 cm from the bottom of the test channel. Figure 8 shows 13 measuring points on subchannel cross section. Measurements are made 4 times at each measuring points so that the total measuring times are 16 seconds. Measurements of each experimental set are performed under varing flow rate and inlet temperature of subchannel.

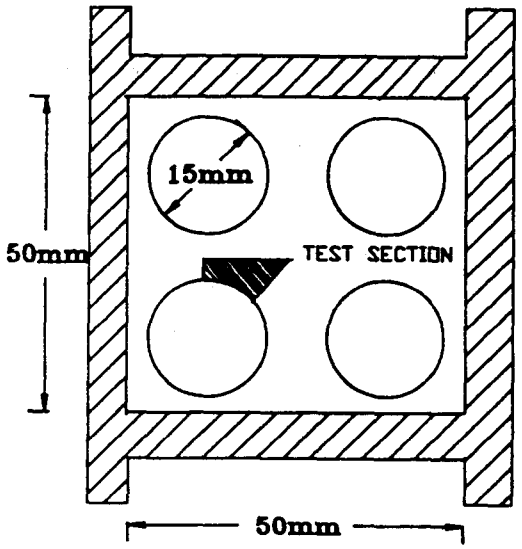

Fig. 8. Measuring Point on Subchannel Cross Section

6.2. Experimental procedure

The experimental procedures are as follows;

1) Installation of double conductivity probes on subchannel wall and calibration of manometer
2) Heating of coolant until steady state is reached at adjusted flow condition
3) If steady state is attained, measurements of void fraction and vapor velocity are performed 4 times at each position traversing conductivity probe
4) Adjust inlet temperature and mass flow rate and repeat above procedures 2 & 3
5) Calculation of slip ratio, flow quality, superfi cial velocity and distribution parameter C_o by VAC

7. Experimental results and analysis

In these experiments, liquid velocity distribution is not measured directly on the channel cross section and so major parameters are calculated by average liquid velocity calculated from measured mass flow rate at subchannel entrance.

7.1. Variation of C_o according to flow conditions

It is known that distribution parameter C_o, which accounts for local relative velocity between two phases and void distribution, is only a function of flow pattern.[1] Generally, the flow pattern is a function of average void fraction and so C_o is formulated as a function of average void fraction in this research. Distribution parameter C_o is less than 1 at subcooled boiling and C_o converges to 1 as average void fraction increases. Figure 9 shows the relation between distribution parameter C_o and channel averaged void fraction. Average void fractions of experiments are varied from 5% to 14 % and system pressure is maintained less than 3 atmospheric pressure. At low system pressure as in this study, the vapor velocity is affected more by the buoyany force resulted from density difference than by the inertia force of liquid phase so that C_o is larger in the subcooled region than at high pressure. Empirical correlation C_o is obtained as a function of average void fraction by best fitting as,

$$C_o = 0.000944001\ \alpha^3 - 0.0315899\ \alpha^2 + 0.319653\ \alpha + 0.00324523$$

where $0 \leq \alpha \leq 14.5$ (%)
Pressure $\leq$ 3 atmospheric pressure

Figure 10 shows the variation of C_o according to flow quality, that is, C_o increases as flow increases.

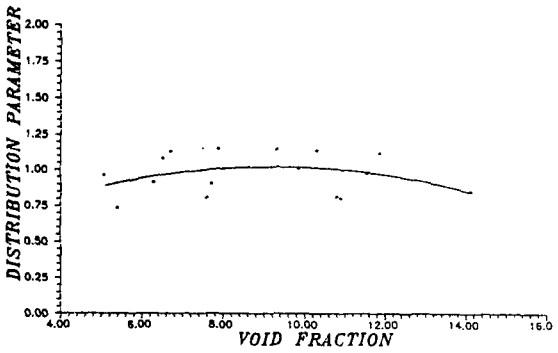

Fig. 9. The Variation of C_o According to Average Void Fraction

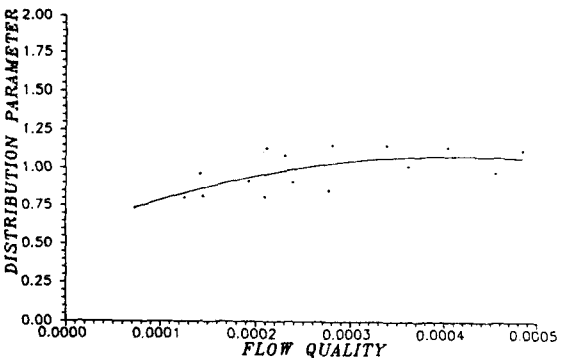

Fig. 10. The Variation of C_o According to Flow Quality

7.2. Relation between average void fraction and vapor velocity

Figure 11 shows the variation of slip ratio as the average void fraction. The result reveals that the slip ratio will increase according as the void fractions increase at subcooled boiling.

The vapor size affects the vapor velocity. Figure 12 shows that the larger the vapor size, the higher the vapor velocity. It shows that the vapor velocity is affected more by the buoyancy force than by the drag force at low pressure.

Also as void fraction increases, superficial vapor velocity increases and superficial liquid velocity will decrease. The results shows the changes of superficial velocity is affected more by the average void fraction than by the velocity of each phase according to the degree of subcooled boiling. It proves that distribution parameter C_o may be regarded as a function of the average void fraction as mentioned. Figure 13 shows this.

Figure 14 shows void fraction, vapor velocity and vapor size distributions. The volumetric mass flow is 1.6. It is shown in Figure 14 that the vapor velocity is higher around the heating rods where the vapor size is larger in the subcooled region.

8. Conclusions

Vapor velocity, void fraction and vapor size distributions in a vertical rectangular subchannel are measured using double conductivity probe. The following conclusions are attained from the results of this study.

(1) The empirical correlation for distribution parameter C_o according to the average void fraction in this vertical rectangular subchannel is as follows

$$C_o = 0.000944001\ \alpha^3 - 0.0315899\ \alpha^2 + 0.319653\ \alpha + 0.00324523$$

where $0 \leq \alpha \leq 14.5$ (%)

Pressure ≤ 3 atmospheric pressure

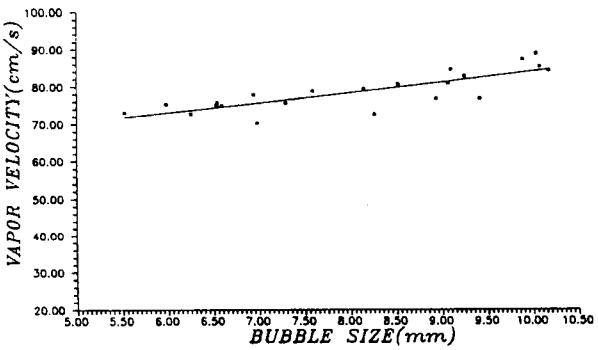

Fig. 12. Relation Between Local Vapor Velocity and Bubble Size

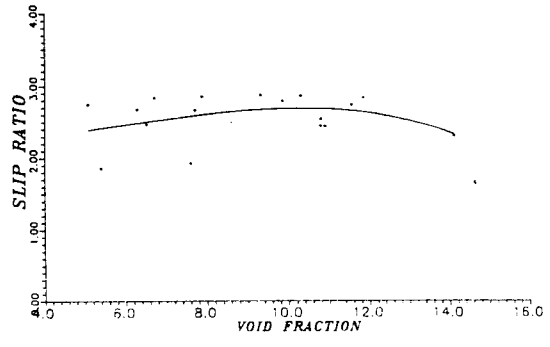

Fig. 11. Variation of Slip Ratio According to Average Void Fraction

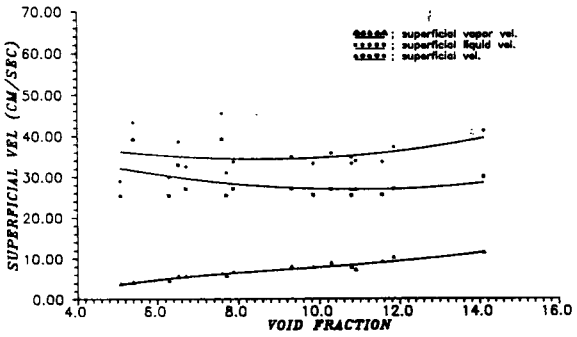

Fig. 13. Superficial Velocity and Average Void Fraction

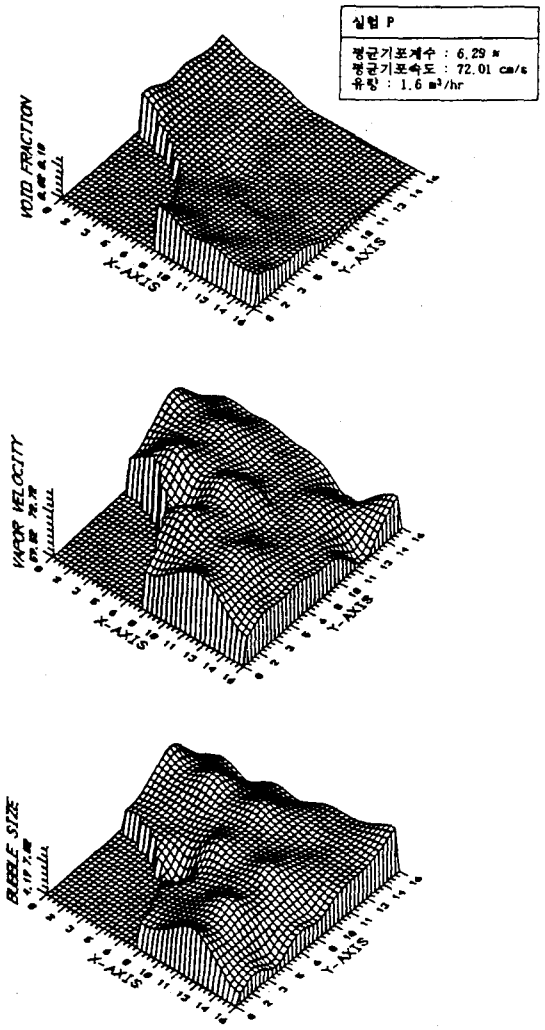

Fig. 14. Distributions of Void Fraction, Vapor Velocity and Vapor Size

(2) Slip ratio increases according as the average void fraction increases at the subcooled boiling

(3) The vapor velocity on the cross section is greatest around the heating rods, whereas the vapor size is largest in the subcooled region.

(4) Using the drift velocity $\bar{V}_{gj}$ to calculate C_o, the variation of vapor velocity is not considered properly as average void fraction varies at low pressure. In order to improve this drawback, the correlation of the drift velocity according to variation of void fraction should be measured simultaneously in the further experiments.

(5) Based on the results of this study, the subjects of the further research are as follows

1) Liquid velocity should be measured and empirical correlation $\bar{V}_{gj}$ should be obtained.

2) Distortions of the void fraction and vapor velocity distributions resulting from the wall effect should be improved by the development of 4×4 bundle geometry

3) The correlation for C_o according to the variation of the void fraction and system pressure should be obtained.

References

1. N. Zuber & J.A. Findlay, "Average Volumetric Concentration in Two-Phase Flow Systems," Journal of Heat Transfer (1965)
2. K. Ohkawa and R.T. Lahley. Jr, "The Analysis of CCFL using Drift-Flux Models," Nuclear Engineering and Design (1980) 3. R.T. Lahley, Jr & F.J. Moody, "The thermal Hydraulics of a Boiling Water nuclear Reactor," American Nuclar Society (1977)
4. B. Chexal et al, "An Assessment of Eight Void Fraction Models for Vertical Flows", NSAC-107 Final Report(1986)
5. B. Chexal et al, "The Chexal-Lellouche Void Fraction Correlation for Generalized Applications," NSAC-139(1991)
6. George P. Nasso, "Development of An Electrical Resistivity Probe for Void-Fraction Measurements in Air-Water Flow," ANL-6738 (1963)
7. D.E. Lamb, F.S. Manning and R.H. Wilhelm, "Measurement of Concentration Fluctuations with An Electrical Conductivity Probe," A.I.Ch.E. Journal (1960)

8. S.G. Bankoff, "A Variable Density Single-Fluid Model for Two-Phase Flow With Particular Reference to Steam-Water Flow," Journal of Heat Transfer (1960)
9. L.G. Neal and S.G. Bankoff, "A High Resolution Resistivity Probe for Determanation of Local Void Properties in Gas-Liquid Flow," A.I.Ch.E. Journal (1963)
10. A.E. Bergles, "Electrical Probes for Study of *Two-Phase Flows*," *Two-Phase Flow Instrumentation* (1969)
11. N. Miller and R.E. Mitchie, "The Development of a Universal Probe for Measurement of Local Voidage in Liquid/Gas Two-Phase Flow *Systems*," *Two-Phase Flow Instrumentation* (1969)
12. G.E. Walmet and F.W. Staub, "Pressure,Temperature and Void Fraction Measurement in Nonequilibrium Two-Phase Flow,"
13. *J.M. Delhaye and G. Cognet, "Measuring* techniques in Gas-Liquid Two-Phase Flows," Springer-Verlag (1984)
14. M. Ishii, "Thermo-Fluid Dynamic Theory of Two-Phase Flow," Eyrolles (1975)
15. *G.F. Hewitt. "Measurement of Two-Phase* Flow Parameters," Academic Press (1978)
16. George C. Barney, "Intelligent Instrumentation," Prentice Hall (1988)
17. W.D Cooper & A.D Helfrick, "Electronic instrumentation and measurementation and Measurement Techniques," Prentice Hall (1985)
18. James W. Dally & William F. Riley & Kenneth G. Mc Connel, "Instrumentation for Engineering Measurements," John Wiley & Sons, Inc (1984)
19. Robert F. Couhhlin & Frederick F. Driscoll, "Operational Amplifiers and Linear Integrated Circuits," Prentice Hall (1982)
20. 윤병조, "수직 사각 유로 내에서의 기포계수 측정에 관한 연구", 석사 학위논문,서울대학교 (1991)
21. 김경환, "수직 사각 유로내에서의 기포속도 및 분포 측정에 관한 연구," 석사 학위논문,서울대학교 (1992)
22 전자기술 연구회편, "센서와 전자회로," 기문사 (1989)
23. Akami Serizawa et al, "Turbulence Structures of Air-Water Bubbly Flow,"Int. J. Multi Phase *Flow, Vol.2 pp 221-233 (1974)*